

# An investigation on the fine defect structure of CoCrTa/Cr magnetic thin films

Bunsen Y. Wong, Yong Shen, and David E. Laughlin

*Data Storage System Center, Department of Materials Science and Engineering, Carnegie Mellon University, Pittsburgh, Pennsylvania 15213*

(Received 5 June 1992; accepted for publication 23 September 1992)

The fine defect structure inside the CoCrTa grains in a CoCrTa/Cr bilayer film has been investigated by high-resolution transmission electron microscopy. A high density of stacking faults bound by partial dislocations has been observed. The origin of these stacking faults and the nucleation and growth of CoCrTa on Cr columns have been discussed. It is suggested the surface morphology of the Cr column could play an important role in determining the number of CoCrTa nuclei and consequently the size of the individual CoCrTa crystallographic variants. In addition, plates of face-centered cubic CoCrTa separating the hexagonal-close-packed regions have been found and we believe that the existence of these plates could lead to coercivity enhancement.

## INTRODUCTION

The progressive quest for higher areal bit density in magnetic recording has prompted extensive research and development in longitudinal thin-film media. The relationship between the structure and the magnetic properties of Co-based alloy (Co)/Cr bilayer thin-film media has often been studied in attempts to improve media performance. As a result, the effects of crystallographic texture,<sup>1-3</sup> grain size, microstructure,<sup>4,5</sup> element segregation,<sup>6,7</sup> morphological isolation,<sup>8,9</sup> etc. on the magnetic properties have been well documented. However, the fine structure inside the individual Co grains has for the most part been unexplored. Previous works<sup>10-12</sup> have observed a high density of striations in the high coercivity CoCrPt, CoCrTa/Cr etc. thin films. These striations have been determined to be (0001) stacking faults (SFs),<sup>10,12</sup> but their nature and origin remain unresolved. A detailed understanding of the microstructure within the Co grain structure is essential because the defect concentration and the crystal homogeneity will affect the magnetic properties and ultimately, the recording performance.

High-resolution transmission electron microscopy (HRTEM) presents the best available means to study the fine structure inside the Co grains. The cross section and the interfacial structure of CoNiCr/Cr thin films have been studied with HRTEM,<sup>13</sup> whereas similar studies on plane view specimens have not been proven to be successful.<sup>11,14</sup> This is because the normal transmission electron microscopy (TEM) specimen thinning procedure, i.e., ion milling, cannot completely remove the Cr underlayer and provide a large thin area of Co for observation. The scattering of the electron wave by the Cr underlayer thus impairs the phase contrast of the Co layer. Consequently, it has not been possible to study the atomic structure of Co grains in such TEM specimens. In our present work, this problem has been solved by preparing the plane view specimen with a jet-polishing technique (see next section). Large thin areas of the CoCrTa layer were thereby obtained and this

allows the atomic structure of the CoCrTa grains to be studied by HRTEM.

## EXPERIMENTAL PROCEDURES

An 800 Å Co<sub>82.8</sub>Cr<sub>14.6</sub>Ta<sub>2.6</sub>/2500 Å Cr bilayer film was sputtered onto a mechanically textured NiP/Al substrate at 260 °C. The deposition was carried out in a LH Z-400 sputtering system by rf diode sputtering. A deposition rate of 20 Å/min was used for both the Cr and CoCrTa in order to enhance grain growth and crystal perfection. The base pressure in the deposition chamber was  $7 \times 10^{-7}$  Torr and an argon sputtering gas pressure of 5 mTorr was employed. Disks, 3 mm in diameter, were punched out from the specimen and the NiP substrate was thinned by mechanical lapping. Final thinning of the NiP substrate and the Cr underlayer was carried out by jet polishing. The polishing solution consisted of 15% butanol, 65% ethanol, and 20% perchloric acid by volume. The initial polishing condition was set at 30 V and 40 mA and the final polishing was carried out at 20 V and 25 mA with a solution temperature between 0 and -5 °C. The specimens were studied by transmission electron microscopy using a JEOL 4000EX high-resolution electron microscope.

## RESULTS AND DISCUSSION

Figure 1 shows a bright field (BF) image and the corresponding selective area diffraction (SAD) pattern of the CoCrTa film. The average grain size was measured to be 36 nm. A high density of striations can be seen inside the CoCrTa grains. These are observed by viewing the SFs edge on. Since the specimen was deposited at 260 °C, the Cr underlayer should have acquired a [100] fibrous texture, which in turn should induce a [1120] fibrous texture in the CoCrTa layer.<sup>2</sup> The orientation relationship between the CoCrTa and the Cr grains is that of Pitsch-Schrader:  $(11\bar{2}0)_{\text{CoCrTa}} \parallel (100)_{\text{Cr}}$ ,  $[0001]_{\text{CoCrTa}} \parallel [011]_{\text{Cr}}$ .<sup>15</sup> In other words, the (1120) CoCrTa planes and the (100) Cr planes

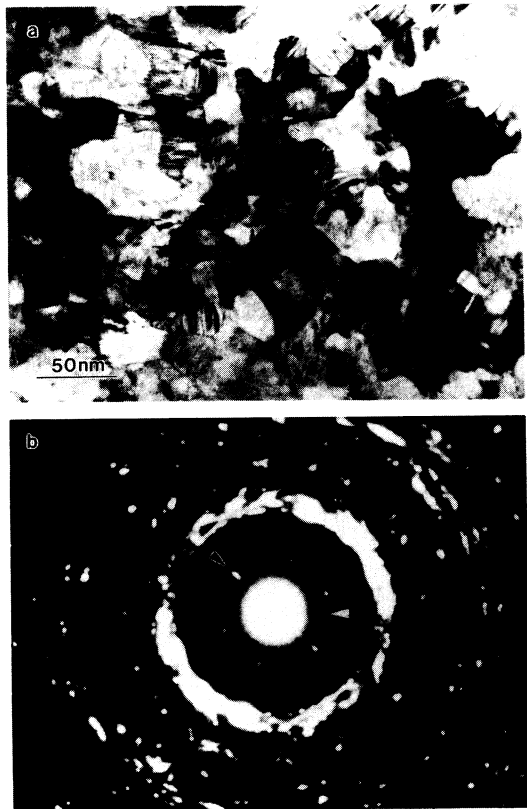


FIG. 1. (a) A BF image of a  $[11\bar{2}0]$  textured CoCrTa film. (b) Corresponding SAD pattern.

are parallel to the plane of the film. Hence, the  $c$  axes of the CoCrTa grains lie in the plane of the film and the (0001) SFs are perpendicular to them. The presence of SFs is also manifested in the SAD pattern [Fig. 1(b)], in which streaks caused by these planar defects can be observed (black arrow). Moreover, the strong  $c$  axes in-plane texture is revealed by the presence of the double diffracting (0001) ring (white arrow). The random orientation of the striations indicates that the  $c$  axes are randomly arranged in the plane of the film and that there is no preferred alignment of the  $c$  axes along the mechanical texture lines. No Cr diffraction rings can be observed in the SAD pattern indicating that the Cr underlayer has been completely removed.

Figure 2 shows the HRTEM image of a  $[11\bar{2}0]$  CoCrTa grain. Two crystallographic variants, with their  $c$  axes normal to each other, are present. The origin of the two variants has been discussed in an earlier article.<sup>12</sup> The disparity in the volume fraction could have been caused by the surface roughness of the Cr column on which the CoCrTa grew. This roughness exists locally in the form of ledges or atomic steps on Cr(100). Nucleation of CoCrTa will start at such ledges because the interfacial energy can be significantly reduced. This implies that the number of nuclei would thus depend on the surface morphology or the density of ledges of the Cr column. Hence, the character of such ledges could very well determine which variant would become dominant because the interfacial structural

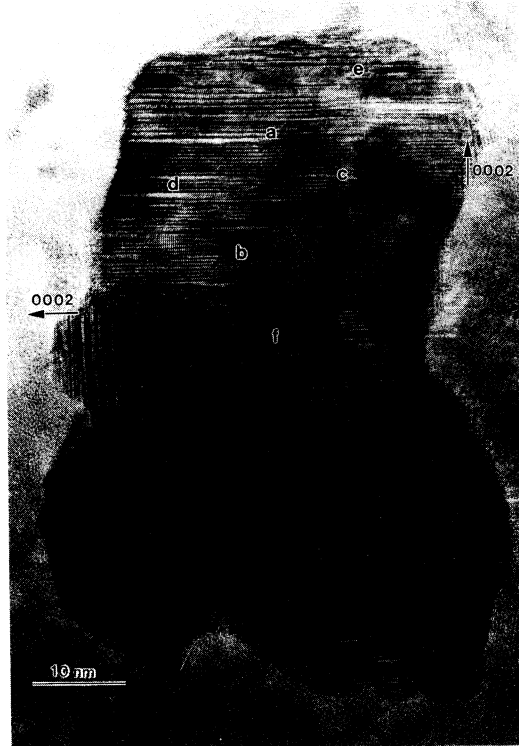


FIG. 2. A HRTEM image of a  $[11\bar{2}0]$  grain.

energy could be minimized by the nucleation and growth of a specific variant.

Upon closer observation, it can be observed that the (0001) planes in the top half of the dominant variant are not parallel to those in the bottom half but there is a  $2.5^\circ$  rotation between them. Simulation results<sup>16</sup> of the interfacial structure of the two crystals in the Pitsch-Schrader orientation relationship have shown that a  $1^\circ$  rotation between Co [0001] and Cr[011] in the interface will lead to a more energetically favorable interphase boundary. The rotation in Fig. 2 thus implies that there was more than one nucleating site when CoCrTa was growing on Cr(100). This is because each nucleus will undergo a rotation with respect to Cr(100) in order to achieve better matching. If the sense of rotation is different for the two nuclei, a  $2^\circ$  rotation will exist between their (0001) planes. This is shown in Fig. 3(a) which is a magnified image of region **a** in Fig. 2. A  $2.3^\circ$  rotation was measured between the (0001) planes from the left and the right which indicates that the two regions originated from two different nuclei. The above results show that there is actually more than one CoCrTa nucleation site. Under the present focusing condition, only the (0001) and  $(10\bar{1}0)$  planes can be resolved [Fig. 3(b)].

Figure 4 shows the magnified images of regions **b** and **c** in Fig. 2. In both figures, the stacking between the top and the bottom regions is different, thus resulting in SFs. They are separated by a Burger's vector of the type  $1/6\langle 11\bar{2}0 \rangle$ . It can be seen from Fig. 2 that the average spacing between the SFs is about 7 (0001) planes. A large amount of dislocation contrast,<sup>17</sup> similar to that shown in

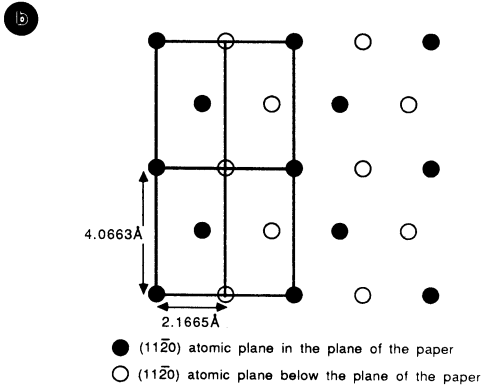


FIG. 3. (a) HRTEM image of area a in Fig. 2 (b) Schematic showing the atomic column structure along the  $[11\bar{2}0]$  zone axis.

Fig. 5, can be observed throughout the grain. These are the bounding partials of the SFs since they are found at the end of the SFs.

There are two possible origins of the SFs. First of all, they could have been created by the thermal stress that was generated due to the difference in the coefficient of thermal expansion between CoCrTa and Cr. When this stress exceeds the critical shear stress for slip in the  $(0001)$  plane, a partial dislocation with a Burger's vector  $1/6\langle 11\bar{2}0 \rangle$  will slip on the  $(0001)$  plane resulting in a deformation SF. On the other hand, the SFs could simply be growth faults due to misplacement of atoms during the nucleation and growth of CoCrTa. Previous TEM studies<sup>16</sup> have shown that the SF density increases with substrate temperature up to 260 °C. However, further enhancement in substrate temperature produces a decrease in the number of SFs and also leads to the growth of the face-centered-cubic (fcc) phase. Hence, it is unlikely that the SFs are produced by thermal stress since the density should increase with substrate temperature. On the other hand, the density of growth SFs will exhibit a maximum at the hexagonal-closed-packed (hcp)  $\rightarrow$  fcc transformation temperature because at that temperature the SF energy is minimum.<sup>18,19</sup> Above this temperature, nucleation and growth of the high-temperature phase, i.e., fcc, will become more energetically favorable. Equilibrium bulk phase diagrams have shown that the addition of Cr and Ta suppresses the fcc  $\rightarrow$  hcp transformation temperature below 422 °C, the transformation temperature of pure Co. Hence, a substrate tempera-

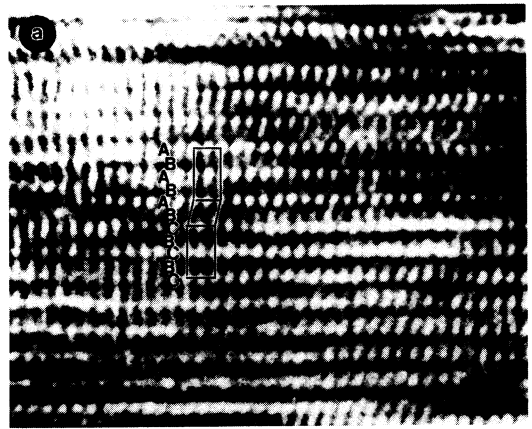


FIG. 4. (a) & (b) HRTEM images of area b and c in Fig. 2. The stacking sequence in both sides of the stacking faults is shown.

ture of 260 °C could very well be in the vicinity of the transformation temperature, thus making growth of the SFs easier. We therefore conclude that the SFs are most likely growth faults.

A SF can be regarded as a thin region of fcc CoCrTa. Thicker plates of the fcc phase have also been found in the grain such as those in region e and f (Fig. 6). They extend across the entire grain, thus effectively separating regions



FIG. 5. HRTEM image of area d Fig. 2 showing a SF bounding partial dislocation (arrow).



FIG. 6. (a) & (b) HRTEM images of areas e and f in Fig. 2 respectively. The atomic stacking sequence shows that the structure is fcc.

of hcp CoCrTa. The magnetic anisotropy of fcc Co is lower than that of the hcp phase by more than one order of magnitude<sup>20</sup> and it is essentially a weak ferromagnetic phase. Hence, these faulted regions could possibly decrease the exchange coupling within the grains, leading to an enhancement of the coercivity. This is similar to the coercivity mechanism in the CoP alloy in which Co is surrounded by CoP<sub>2</sub>, a weak ferromagnet.<sup>21,22</sup> Moreover, the SFs could also give rise to composition inhomogeneity due to the Suzuki effect,<sup>23,24</sup> which describes the segregation of solute atoms to the SF. Consequently, the nonmagnetic Cr and Ta atoms may help decouple the hcp regions within the grain and result in higher coercivity.

## CONCLUSIONS

We have successfully removed the Cr underlayer during TEM specimen preparation and obtained a CoCrTa

film with a  $[11\bar{2}0]$  texture. The CoCrTa fine grain structure has been studied by HRTEM. The existence of two crystallographic variants growing on one Cr grain has been confirmed. A high density of stacking faults, bound by partial dislocations, can be found in both variants throughout the grain. It has been shown that these are most likely growth faults and that their density is closely associated with the substrate temperature. A slight rotation between (0001) planes in different regions of the grains has also been observed. This is due to the fact there was more than one CoCrTa nucleus growing on the Cr grain. Finally, plates of fcc CoCrTa separating the hcp regions have been also found.

## ACKNOWLEDGMENTS

This research is based upon work supported by the National Science Foundation under Grant No. ECD-8907068. The government has certain rights in this material. Dr. Y. Shen was supported by a grant from Hitachi Metals Ltd. We would also like to acknowledge Dr. P. Frausto of Tosoh SMD, Inc. for donating the target material.

- <sup>1</sup>J. Daval and D. Randet, *IEEE Trans. Magn.* **MAG-6**, 4733 (1970).
- <sup>2</sup>S. L. Duan, J. O. Artman, B. Wong, and D. E. Laughlin, *IEEE Trans. Magn.* **MAG-26**, 1587 (1991).
- <sup>3</sup>M. Ishikawa, N. Tani, T. Yamada, Y. Ota, K. Nakamura, and A. Itoh, *IEEE Trans. Magn.* **MAG-22**, 573 (1986).
- <sup>4</sup>T. Chen, T. Yamashita, and R. Sinclair, *IEEE Trans. Magn.* **MAG-17**, 3187 (1981).
- <sup>5</sup>T. Lin, *J. Magn. Magn. Mater.* **86**, 159 (1990).
- <sup>6</sup>Y. Maeda and M. Asahi, *J. Appl. Phys.* **61**, 1972 (1987).
- <sup>7</sup>A. Kawamoto, F. Hikami, S. Yasuda, and N. Muto, *IEEE Trans. Magn.* **MAG-27**, 5046 (1991).
- <sup>8</sup>T. Chen and T. Yamashita, *IEEE Trans. Magn.* **MAG-24**, 2700 (1988).
- <sup>9</sup>T. Yogi, T. A. Nguyen, S. E. Lambert, G. L. Gorman, and G. Castillo, *IEEE Trans. Magn.* **MAG-26**, 1578 (1991).
- <sup>10</sup>K. Hono, B. G. Demczyk, and D. E. Laughlin, *Appl. Phys. Lett.* **55**, 229 (1989).
- <sup>11</sup>T. Lin, R. Alani, and D. N. Lambeth, *J. Magn. Magn. Mater.* **78**, 213 (1989).
- <sup>12</sup>B. Y. Wong, D. E. Laughlin, and D. N. Lambeth, *IEEE Trans. Magn.* **MAG-27**, 4733 (1991).
- <sup>13</sup>B. Y. Wong and D. E. Laughlin, *EMSA Proc.* **49**, 760 (1991).
- <sup>14</sup>T. P. Nolan, *EMSA Proc.* **49**, 756 (1991).
- <sup>15</sup>W. Pitsch and A. Schrader, *Arch. Eisenhütt. Wes.* **29**, 715 (1958).
- <sup>16</sup>B. Y. Wong, Ph. D. dissertation, Carnegie Mellon University, 1991.
- <sup>17</sup>M. J. Mills and M. S. Saw, *Proc. Mater. Res. Soc.* **183**, 15 (1990).
- <sup>18</sup>T. Ericsson, *Acta Metall.* **14**, 853 (1966).
- <sup>19</sup>T. C. Tisone, *Acta Metall.* **21**, 229 (1973).
- <sup>20</sup>W. Sucksmith and J. E. Thompson, *Proc. R. Soc. A* **225**, 362 (1954).
- <sup>21</sup>J. S. Judge, J. R. Morrison, D. E. Speliotis, and G. Bate, *J. Electrochem. Soc.* **112**, 681 (1965).
- <sup>22</sup>B. R. Natarajan and E. S. Murdock, *IEEE Trans. Magn.* **MAG-24**, 2724 (1988).
- <sup>23</sup>R. Herschitz and D. N. Seidman, *Acta Metall.* **33**, 1547 (1985).
- <sup>24</sup>H. Suzuki, *J. Phys. Soc. Jpn.* **17**, 322 (1962).